SLAC-TN-04-075
February 4, 2005

TE_{01} High Power Disk Loaded Guide Load*

Z. D. Farkas
Stanford Linear Accelerator Center, Stanford University, Stanford,
CA 94309

Abstract

A method to design a matching section from a smooth guide to a disk-loaded guide, using a variation of broadband matching, [1, 2] is described. Using this method, we show how to design high power loads, attenuators and filters. The load consists of a disk-loaded coaxial guide operating in the TE_{01}-mode. We use this mode because it has no electric field terminating on a conductor, has no axial currents, and has no current at the cylinder-disk interface. A high power load design that has -35 dB reflection and a 200 MHz, -20 dB bandwidth, is presented. It is expected that it will carry the 600 MW output peak power of the pulse compression network. We use coaxial geometry and stainless steel material to increase the attenuation per cell.

Introduction

Although the main focus of this note is on a high power load, this method of broadband matching will also be applied to filters and attenuators. A magnetic stainless steel load using a TE_{11}-mode in a round guide has been developed and implemented [3]. Here we present a load that uses a TE_{01}-mode travelling wave in a disk-loaded guide (DLG). This mode has

- No electric field terminating on a conductor, hence no field emission.
- No axial currents and no axial electric field.
- No currents at the waveguide-disk interface.

Thus, it is expected to have higher average and peak power carrying capacity. The peak magnetic fields, which limits peak power, will be lower. Also, this load, composed of TE_{01} mode cells, does not require brazing, which may cause a reduction of permeability, and hence reduce the attenuation. In order to maximize the bandwidth (BW), the phase advance per cell is $\pi/2$. A bandwidth (BW) in terms of group velocity, v_g, is

$$BW = \frac{v_g[m/\mu s]\Delta\phi_c[cycles]}{L_c[m]} \ . \tag{1}$$

$\Delta\phi_c$ is the range over which the phase advance is nearly linear with frequency. L_c is the length of the cell. A reasonable value for $\Delta\phi_c$ is 1/3 cycles (120 degrees). If $v_g/c = 3.5$ % then BW is 155 MHz. Low group velocity limits BW which is also limited by the necessity to match the disk loaded guide to the input guide.

*Work supported by the Department of Energy, contract DE-AC02-76SF00515

Disk-Loaded Matching Section Theory

We match from a smooth guide to a disk-loaded guide. To obtain a wide bandwidth, the matching is based on a well known design [1, 2], which stipulates $\pi/2$ line lengths whose impedances vary so that the input reflection coefficient, Γ_{in}, is a Butterworth or a Tchebychev polynomial. In our design, the matching $\pi/2$ transmission-line lengths are replaced by $\pi/2$ phase advance disk-loaded cells and their characteristic impedance is replaced by the travelling wave impedance, defined as

$$Z_t = \frac{E^2}{P_t} = (1/v_g)E^2/w \ . \tag{2}$$

E is the maximum electric field P_t is the transmitted power, and w is the energy stored per unit length. Z_t has units of ohms per square meter. Figure 1 shows impedance matching with 90° transmission line sections, (similar to Figure 4.1.4 in reference [2]), and the equivalent matching with 90° phase advance disk-loaded cells. In both cases their impedances are such that the input reflection coefficient to the matching network, Γ_{in}, is a Butterworth or a Tchebychev polynomial.

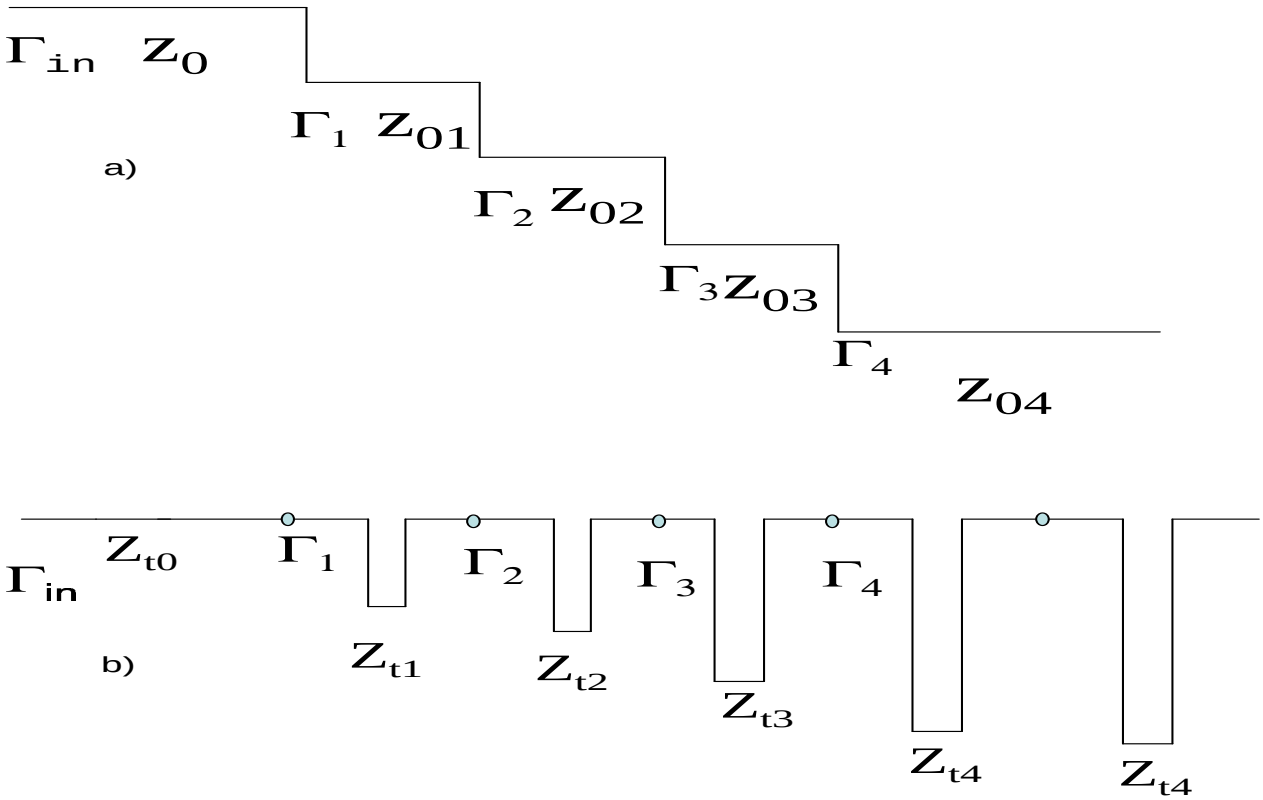

Figure 1: Impedance matching with 90° transmission line sections, and the equivalent matching with 90° phase advance disk-loaded cells.

Choose the number of matching cells, N_m. The number of reflections (discontinuities) is $N_r = N_m + 1$. Choose the reflection coefficient of the first cell, $\Gamma(1)$. Its value is a trade-off between bandwidth and length of the load. The remaining reflection coefficients are given by

$$i = 2, ...N_r, \quad \Gamma(i) = r_\gamma(i) \times \Gamma(1), \tag{3}$$

where $r_\gamma(i)$, are the reflection coefficient ratios, which are binomially distributed so that Γ_{in} is a Butterworth function [2]. The higher the value of $\Gamma(1)$ and the subsequent Γ's, the higher the impedances and the lower the group velocities of the cells. Consequently the attenuation is higher and the load is shorter. But the bandwidth is narrower and the energy densities and fields are higher. The ratio of the impedances, which are also the standing wave ratios (SWR), are:

$$\rho(i) = \frac{1 + \Gamma(i)}{1 - \Gamma(i)} \quad i = 1, 2, ...N_r \tag{4}$$

As we are interested in ratios only, we normalize to the travelling wave impedance of the input guide, Z_{t0}. $Z_{tn} \equiv Z_t/Z_{t0}$. The normalized impedances required for matching are:

$$Z_{tn}(1) = \rho(1), \quad Z_{tn}(i) = Z_{tn}(i-1)\rho(i-1), \quad i = 2, ...N_r. \tag{5}$$

To increase losses we use coaxial geometry. We choose the outer conductor radius r_{out}=2.851 cm, inner conductor radius r_{in}= 0.953 cm and disk thickness t_d = 0.5 cm. At 11,424 MHZ, the TW impedance, the group velocity and the guide wavelength of this coax, obtained with HFSS, are, respectively:

$$Z_{t0} = 35.14 \ \ \text{Mohm/m}^2, \quad v_{g0}/c = 69.6 \ \%, \quad \lambda_{g0}/4 = 0.9445 \ \ \text{cm}.$$

We choose two designs: $\Gamma(1) = 0.16$ and 0.18. For both designs we choose $N_m = 3$, hence the impedance ratios, $r_\gamma = [1 \ \ 3 \ \ 3 \ \ 1]$. Using equations 3 through 5, we find the normalized impedances, Z_{tn}, of the four cells (3 cells required for matching plus the first attenuation cell). A typical coaxial cell and a waveguide cell are shown in Figure 2 a and b, respectively. Frequency vs. phase advance ($\omega - \beta$ diagram) and vs. group velocity for several cells is also shown in Figure 2. Color plots of the electric and magnetic fields, in a 45 degree wedge of a typical cell, are shown in Figure 3.

The disk radii r_a and the cell lengths p_z of the 4 cells are obtained as follows: Use HFSS Driven Solution Ports Only to find λ_g of a smooth cell. Then use HFSS Eigen Mode Solution for a single cell. Start with $r_a = 0$ and $d_{pz} = (\lambda_g/4 - t_d)/2$ and gradually increase r_a. At each r_a, vary d_{pz} till, with a 90 degree phase advance, 11.424 GHz is obtained. Note the impedance and group velocity at each point and construct a table of Z_{tn}, r_a, d_{pz} and v_g. The length of a cell (spacial period) is $p_z = 2d_{pz} + t_d$ where t_d is the disk thickness. The aperture and the maximum aperture are:

$$a_p = r_{out} - r_a - t_d/2, \quad a_{pmax} = r_{out} - r_{in} \ .$$

At the maximum aperture (no disk):

$$\lambda_g = \lambda_{g0}, \quad p_z = p_{z0} = \lambda_{g0}/4, \quad v_g = v_{g0}.$$

Define the normalized apertures and cell lengths as:

$$a_{pn} = a_p/a_{pmax}, \quad p_{zn} = p_z/(\lambda_{g0}/4) \ .$$

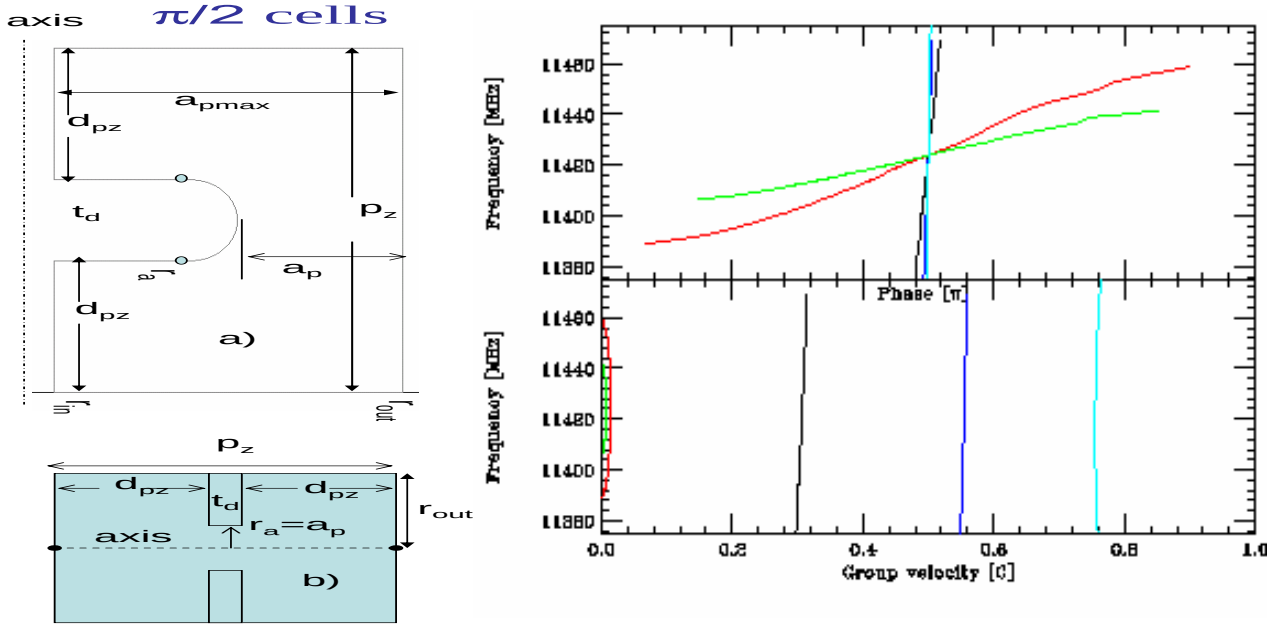

Figure 2: a)Coaxial cell cross section, b) waveguide cell cross section, and Frequency vs. phase advance ($\omega - \beta$ diagram) and vs. group velocity.

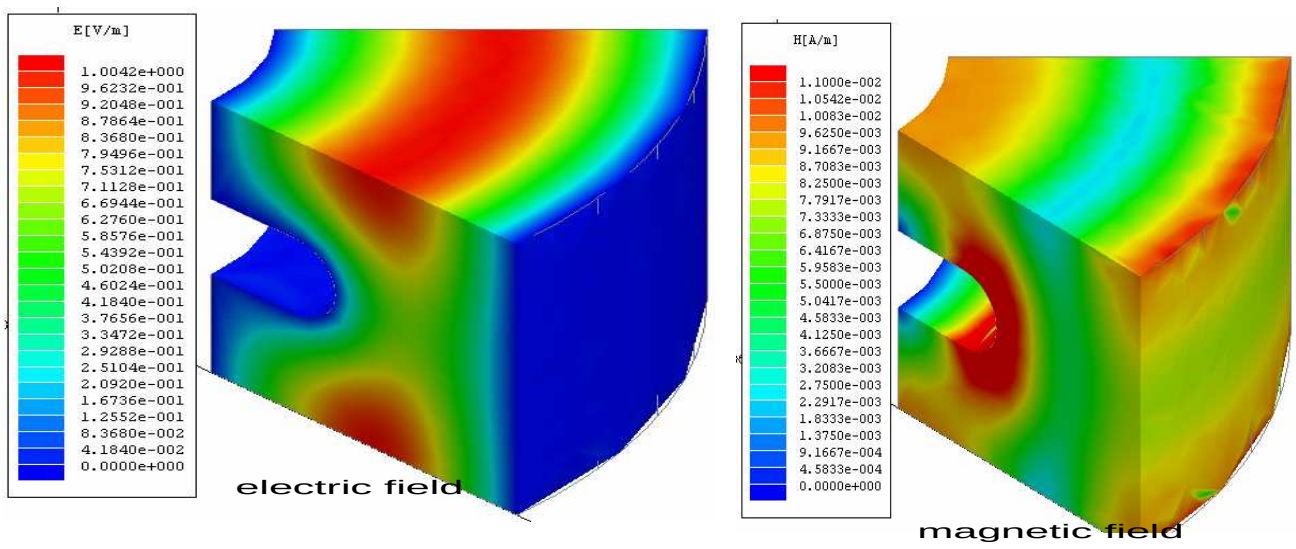

Figure 3: A 45 degree wedge of a typical cell showing electric and magnetic fields. $a_{pn} = 0.593$, $p_{zn} = 1.8$, $v_g/c = 27.9\%$. P=258 nW.

Using the previous equations and the data in the afore mentioned table, obtain polynomials $a_{pn}(Z_{tn})$, $d_{pz}(Z_{tn})$, $v_g(Z_{tn})$. Substitute for Z_{tn} their values required for matching and obtain the aperture, spacial period and group velocity of the 3 matching cells and of the first disk-loaded transmission line cell. These parameters can also be obtained using interpolation. Plots of Z_{tn}, p_{zn} and v_g as a function of a_{pn} are shown in Figures 4a, 4b and 4c, respectively. The input points are denoted circles and the points required for matching are denoted by stars, green for $\Gamma(1) = 0.16$ and blue for $\Gamma(1) = 0.18$.

Cascade the matching cells and add attenuation cells to form a matched disk-loaded transmission line. The parameters of the attenuation cells can vary but only adiabatically. The distances between the disks are

$$d_c(i) = d_{pz}(i) + d_{pz}(i+1), \quad i = 1...N_t - 1 \ . \tag{6}$$

N_t is the total number of disks. In the above procedure, after changing the aperture of the cells, they are tuned by changing their lengths, rather than in the conventional way by changing their outer radii. The parameters of the smooth coax to the disk-loaded coax match, for $\Gamma(1) = 0.16$, are listed in Appendix A, Table 1.

$\mathbf{TE_{01}}$ High Power Load

To make a load, we add to the matching cells a sufficient number of attenuation cells to decrease the input reflection (return-loss) to an acceptable level and terminate the last attenuation cell with a short circuit. The distance between the last disk and the end short is not crucial. The length of the load depends on the attenuation per cell which is given by

$$\alpha_c = \frac{p_z \pi f}{Q \ v_g} \ \text{ nepers} \ . \tag{7}$$

To increase the attenuation per cell (to make the load shorter) and to distribute the power dissipation more evenly, the group velocities, hence the apertures, are monotonically decreased by small amounts. Here we linearly increased r_a by $\Delta r_a = 0.15$ mm. From data of r_a, d_{pz} and v_g of cells that have $\pi/2$ phase advance at the operating frequency, (obtained with HFSS or SMART2D or other codes) we obtain polynomials $p_z(r_{an})$ and $v_g(r_{an})$ of the attenuation cells. The normalized lengths of the cells and their group velocities are plotted in Figures 5a and 5b, respectively, as a function of normalized aperture. The input points are denoted circles and the points required by the attenuation cells are denoted by stars. The solid lines are plots of the fitted polynomials. The distances between the disks are given by Equation 6.

For $\Gamma(1) = 0.16$, sixteen attenuation cells are sufficient to reduce reflection to an acceptable level. For this load, line plots of the electric field at r=1.8 cm, and the magnetic field at $r = r_{in}$ are shown in Figure 6 a and b, respectively. A color plot of the electric field is shown in Figure 6, c and of the magnetic field in Figure 6, d. The input power is 100 MW. The reflections, s_{11} and the SWR are shown in Figure 7. The above plots were obtained using HFSS. r_a and d_c are inputs to HFSS.

To connect the coax to a TE_{10} rectangular guide we can use a Wraparound Mode Converter(WMC) [5], which converts RF signals from the TE_{10} mode in rectangular guide to the TE_{01} mode in round guide. This has the advantage that the inner conductor can be secured at both ends. But a WMC limits the input power, therefore the load has to have a waveguide input. For testing the load at

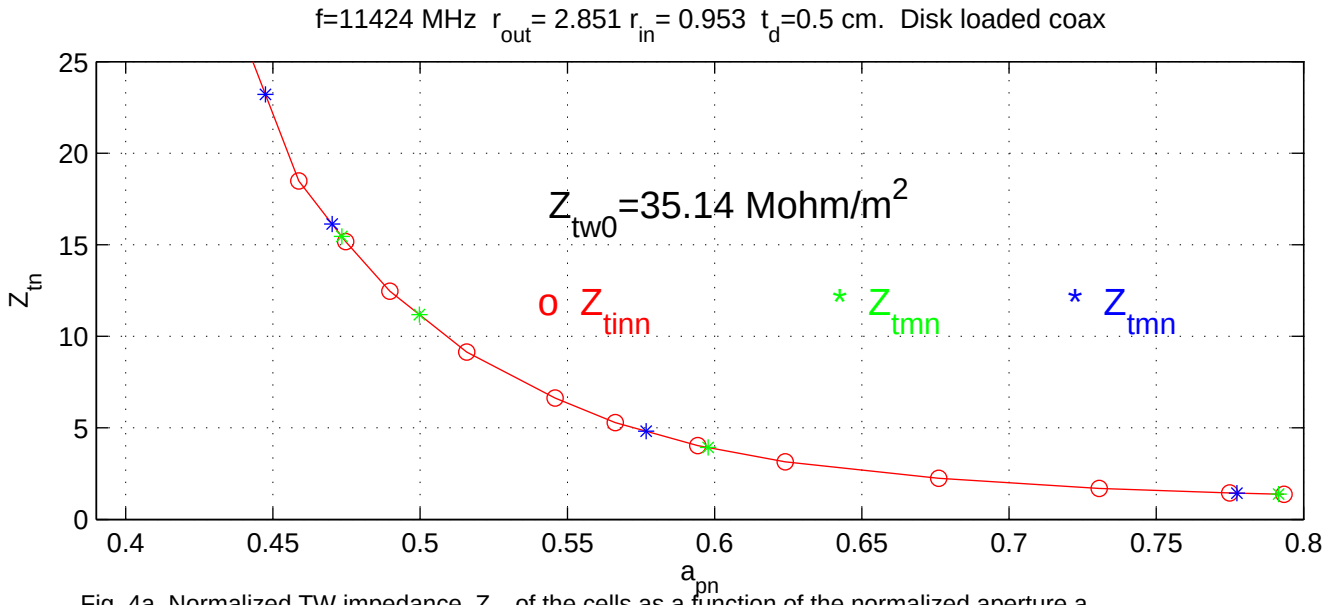

Fig. 4a. Normalized TW impedance, Z_{tn}, of the cells as a function of the normalized aperture a_{pn}.

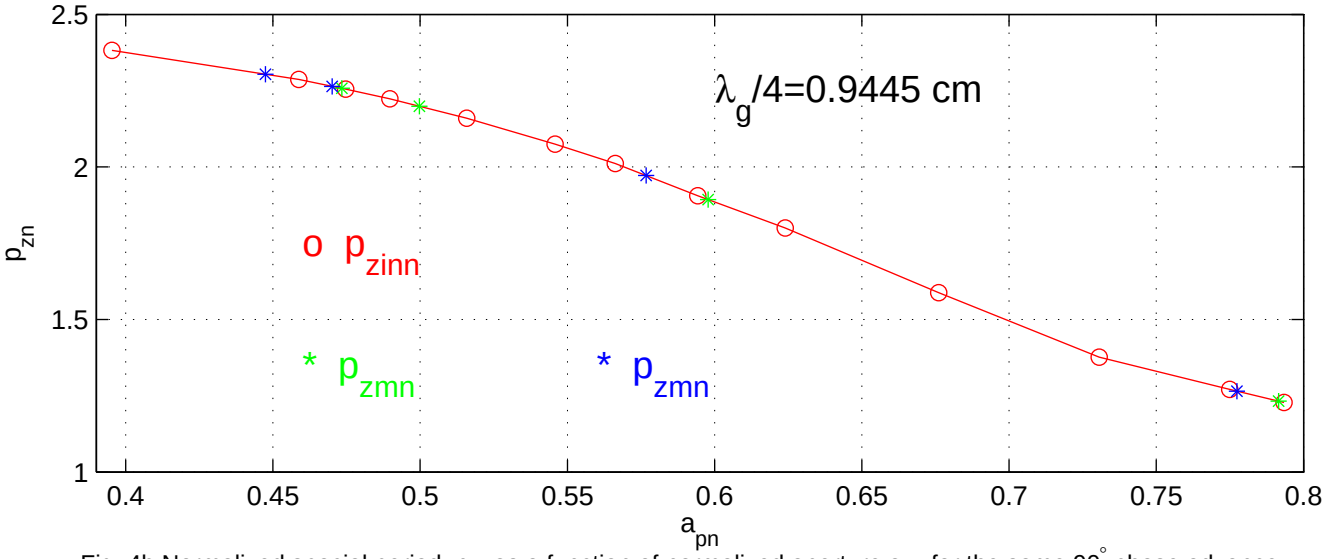

Fig. 4b.Normalized spacial period, p_{zn} as a function of normalized aperture a_{pn} for the same 90° phase advance.

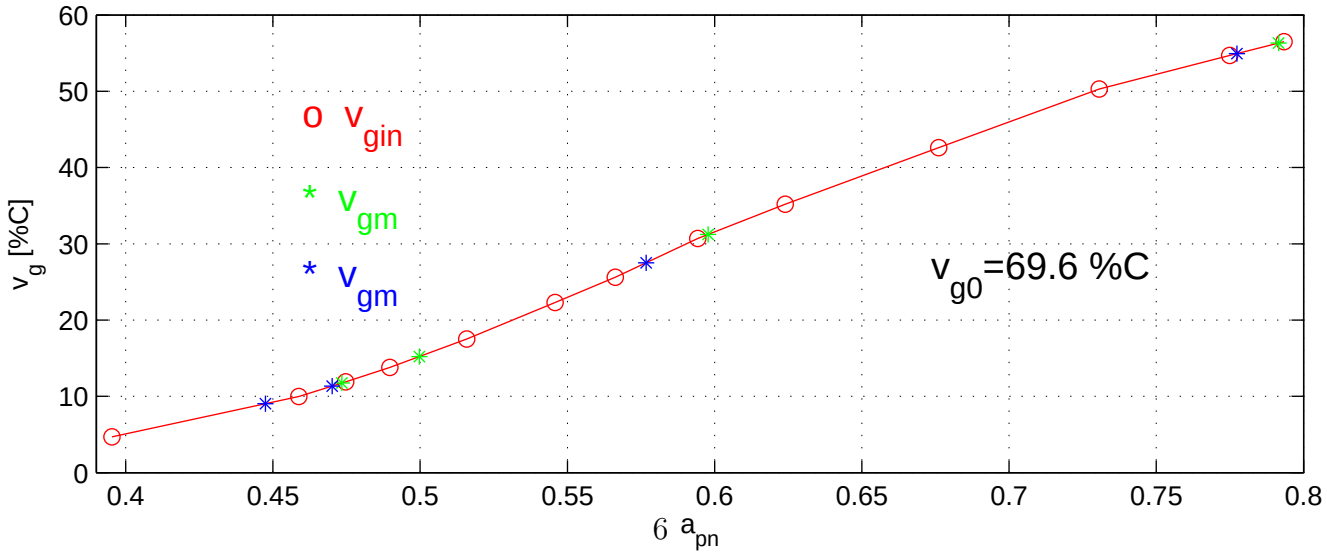

Fig. 4c. Group velocity, v_g as a function of normalized aperture a_{pn} for the same 90° phase advance.

Figure 4: Impedance, cell length and group velocity vs. normalized aperture

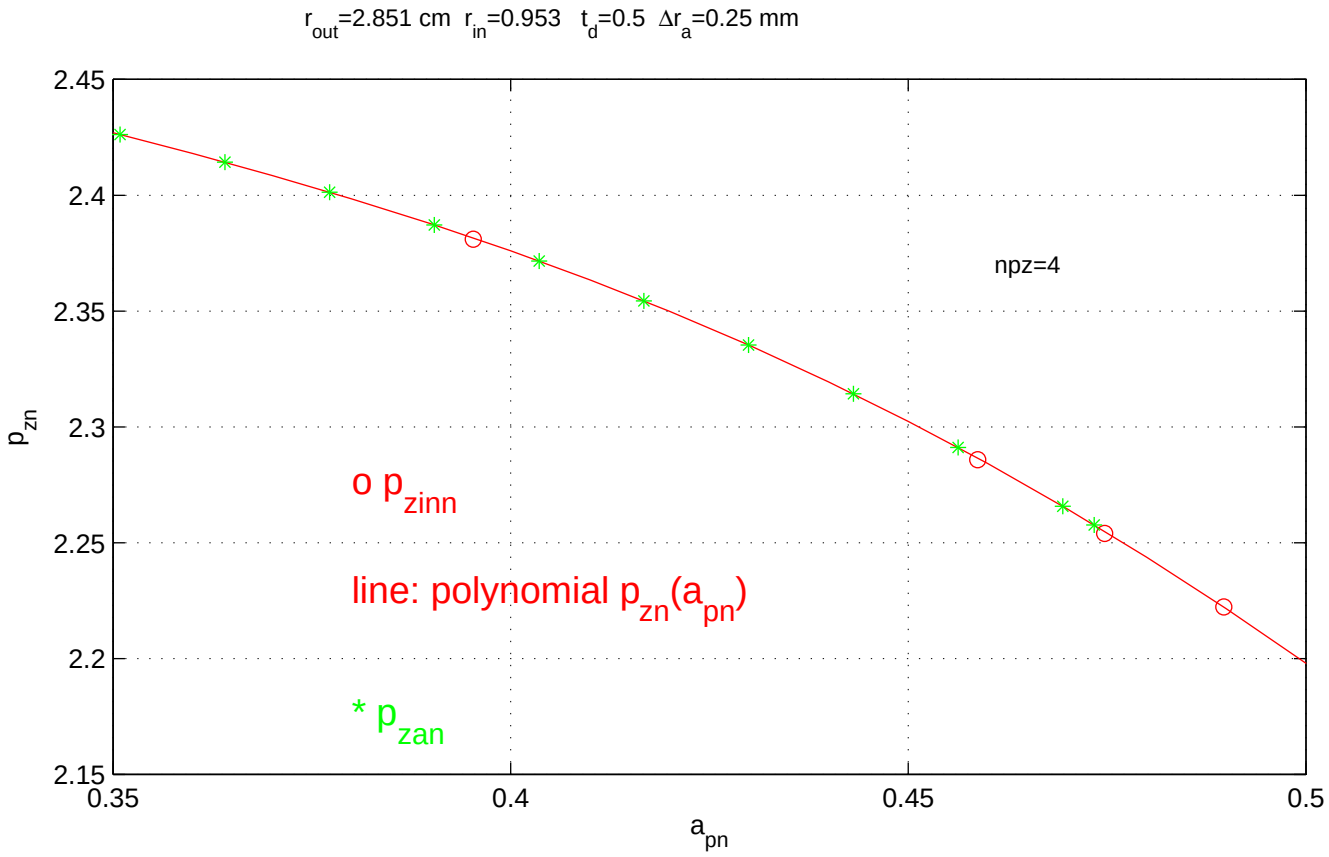

Fig. 5a. Spacial period, p_{zn} as a function normalized aperture a_{pn} for the same 90° phase advance.

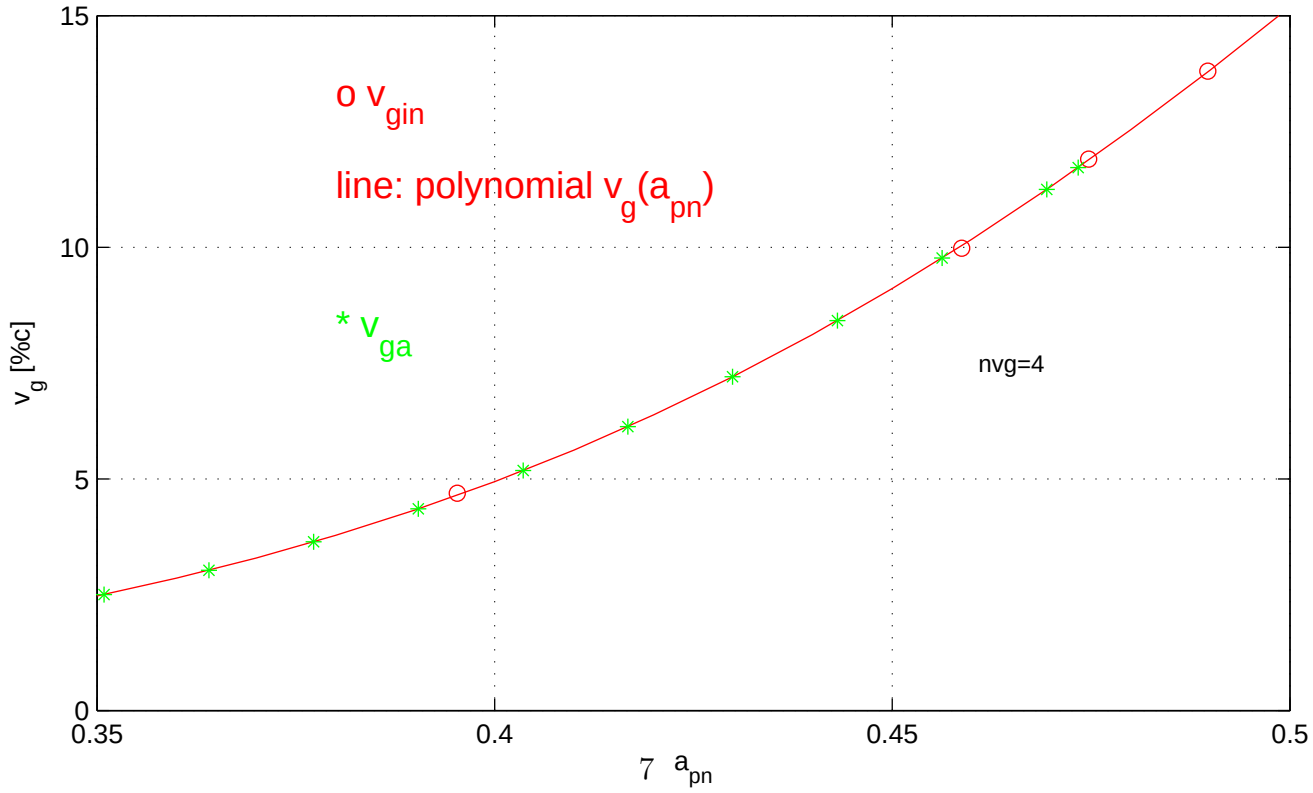

Fig. 5b. Group velocity, v_g as a function normalized aperture a_{pn} for the same 90° phase advance.

Figure 5: Cell length and group velocity vs. normalized aperture

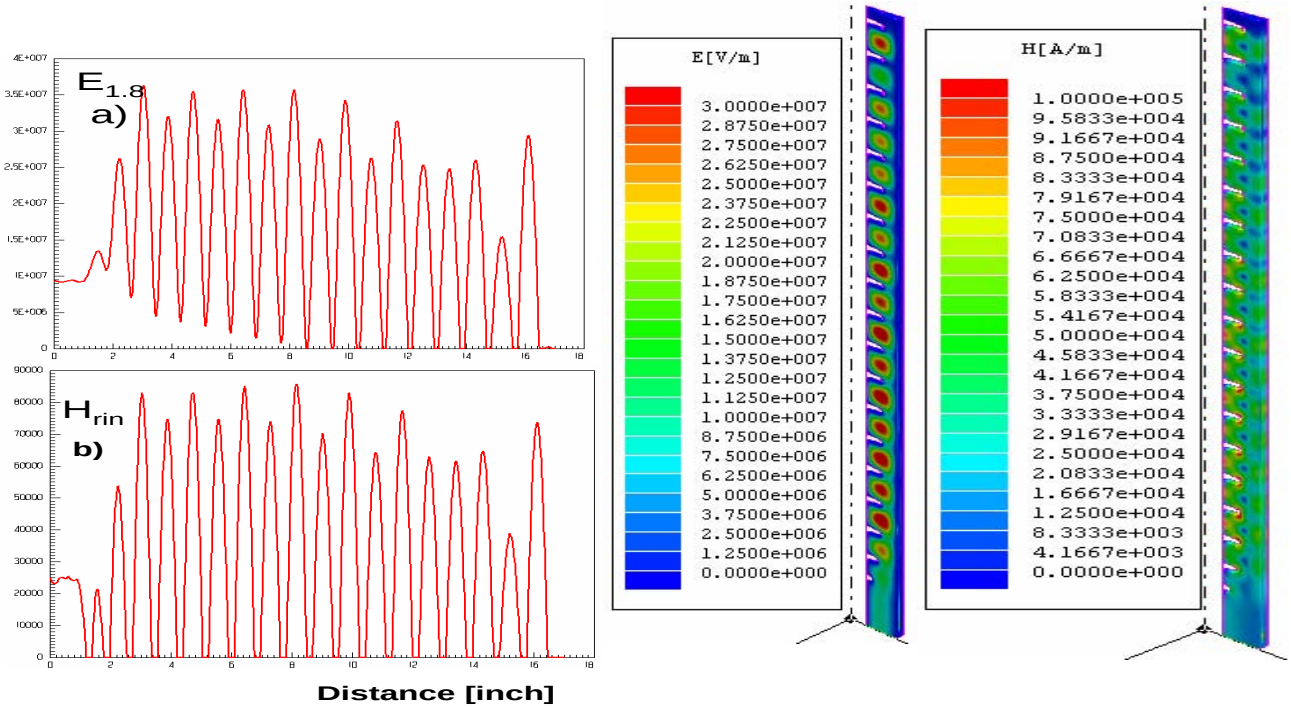

Figure 6: Load, coax input. a) E at r=1.8 cm b) H at $r = r_{in}$ c) E color map d) H color map

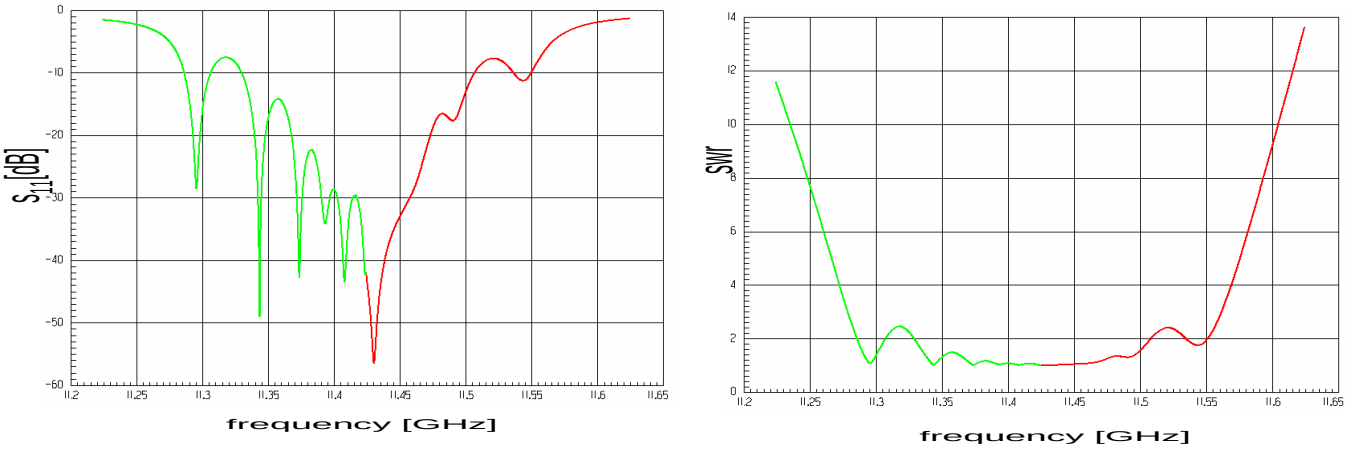

Figure 7: Load, coax input.(a) Reflection (b) SWR. The point at the intersection of the two colors denotes the design frequency of 11.424 GHz

low power, a WMC for 1.5 inch diameter round guide is available. Therefore we design a matching section from 1.5 inch diameter round guide to the coax. First we match the 1.5 inch diameter guide to a guide having the same diameter as the outer conductor of the coax. Then we match this guide to the coaxial guide. The inner conductor of the coax ends in a hemisphere. The parameters of the match from 1.5 inch diameter waveguide to smooth coax are listed in Appendix A, Table 2. Color plots of the electric and magnetic fields in this wave guide to coax matching section are shown in Figure 8 a. Its input reflection as a function of frequency is shown in Figure 8 b. In the figure the power input to a full circle is 100 MW. Similar plots for a somewhat different design where the inner conductor terminates in a square rather than in a hemisphere are shown in Figure 9. It shows that the fields are about the same as with the hemisphere termination.

We connect the waveguide to coax matching section to the coax input load to form a load with 1.5 inch diameter waveguide input. Line plots of the electric field at r=1.8 cm, and the magnetic field at $r = r_{in}$ are shown in Figure 10, a, and b respectively. A color plot of the electric field is shown in Figure 10 c and of the magnetic field in Figure 10 d. The input power of 100 MW. The reflection, s_{11}, and the SWR are shown in Figure 11. The parameters of this load are listed in Appendix A, Table 3. Plots similar to those shown in Figure 10 are shown in Figure 12 for $\Gamma(1) = 0.18$.

Reflections vs. frequency for both designs are shown in Figure 13. These two designs illustrate the trade-off between bandwidth and length. For $\Gamma(1) = 0.16$, the -10 dB bandwidth is 350 MHz and the disk-loaded coax is 17 inches long. For $\Gamma(1) = 0.18$, the -10 dB bandwidth is 250 MHz and the disk loaded coax length is 12.8 inch. For $\Gamma(1) = 0.16$, for an input power of 100 MW, the maximum electric field is 30 MV/m, and the maximum magnetic field is 0.1 MA/m. This magnetic field is about a third of the field in the present load, hence its power carrying capacity should be nine times greater. For both designs, the maximum surface electric field is zero. For $\Gamma(1) = 0.18$, the magnetic field increases by about 20%.

The input average power is $P_{ia} = P_{ip}T_p f_{rep}$, where P_{ip} is the input power, T_p is the pulse width, f_{rep} is the pulse repetition frequency. If $P_{ip} = 100$ MW, $T_p = 400$ nS, $f_{rep} = 120$ Hz, then, $P_{ia} = 4.8$ KW.

We assumed that the stainless steel has a $\sigma = 1,122,000$ mhos/m, and $\mu_r = 11$. The Q's of the cells, given by HFSS, are about 500. The imaginary frequency, $f_{im} = f_{re}/2Q \approx 11.4$ MHz. For the first design, the length of the load is 52 cm and of the coax 43 cm. A view of the load is shown in Figure 14.

By putting a thin conducting plane along the diameter of the guide we increase the attenuation per cell and thereby shorten the load, but then, E-fields will terminate on a conductor. The advantage of zero axial currents still remains.

TE_{01} Test Structure

We test the matching section, by terminating it with its mirror image to form a test structure as shown in Figure 15 a. The distance between the first attenuation disk and its mirror image disk

$$d_c(N_r) = 2 \times d_{pz}(N_r) \ . \tag{8}$$

Line plots of the electric field at r=1.8 cm, and the magnetic field at $r = r_{in}$ are shown in Figure 15 b, and c, respectively, for an input power of 100 MW. A color plot of the magnetic field in a 15 degree slice of the coax cylinder is shown in Figure 15 d. Note that there is no magnetic field, hence no current at the inner conductor-disk interface. The reflection, s_{11} is shown in Figure 15 f. The reflection at 11,424 MHz is -40 dB.

Because the code SMART2D [4] is faster than HFSS, we use it to show how the reflection varies due to small perturbation in geometry and how the band width varies with group velocity. SMART2D works with a square-tip disks. But if we know r_a of a round-tip disk we can obtain the equivalent r_a of a square-tip disk, and vice versa. Plots of reflection and phase of square-tip disk test section are shown in Figure 16 a, for three inner conductor radii of 0.953, 0.943, and 0.963 cm. The plot shows that increasing the inner conductor radius by 0.1 mm changes the center frequency by about 0.2%, 23 MHz. The reflection and transmission for three group velocities are plotted in Figure 16 b. The plots illustrate how the bandwidth increases and attenuation decreases as the group velocity increases.

TE_{01} Bandpass Filter

The test structure turns out to be a band-pass filter. For such use, it would be made of copper and have a geometry than minimizes the losses. Bandpass filters using TE_{011}-mode coupled cavities have been proposed [6]. The present design is based on a different principle, and should have higher power carrying capacity and higher quality factor. If we make the previously described test section out of copper, it becomes a filter. Its geometry and plots of its reflection and transmission as a function of frequency, are shown in Figure 17.

For a filter we do not wish to increase the loss per cell, therefore we would use a standard disk-loaded guide rather than a coaxial guide. A cross section of a typical waveguide cell is shown in Figure 2 b. Here, r_a is also the aperture. We use a square disk tip which allows us to use SMART2D to obtain the parameters of the cells. We still have to use HFSS to obtain Z_t. An analytic expression for impedance of the input guide is [7]

$$Z_{t0} \equiv \frac{E^2_{\phi max}}{P} = \frac{\eta J_1^2(max)}{0.0948(\lambda/\lambda_g)\lambda_c^2} = \frac{377(0.581^2)}{0.0948(\lambda/\lambda_g)\lambda_c^2} \quad . \tag{9}$$

For our design, r_{out}=1 inch, the analytically obtained Z_{t0} is 0.998 Mohm/m^2 and Z_{t0} obtained with HFSS is 0.999 Mohm/m^2. The waveguide TE_{01} band-pass filter design is similar to the coaxial filter design.

For a second design, we assume that E^2/w is constant, (see eq. 2). Then the ratios of the travelling impedances equal the ratios of the reciprocals of the group velocities.

$$Z_{tn} = Z_{vn} \equiv \frac{1/v_g}{1/v_{g0}} = v_{g0}/v_g \tag{10}$$

Plots for the two designs of Z_{tn}, Z_{vn}, p_{zn} and v_g vs. r_{an} are shown in Figures 18a, 18b and 18c, respectively. Line and color plots of their fields are shown in Figure 19 and Figure 20. Their geometry, their reflection and transmission are shown in Figure 21.

TE_{01} Attenuator

If we place additional attenuation cells in the TE_{01} disk-loaded coax test structure, we have a high power attenuator. With no attenuation cells we have a 2 dB, with 5 attenuation cells a 4 dB and with 7 attenuation cells a 5 dB high power attenuator. The attenuation is about 0.4 dB/cell. Plots of geometry, reflection s_{11} and attenuation s_{12} are shown in Figure 22.

Summary

We have shown how to design loads, filters and attenuators using a variation of broadband matching [1, 2], where $\pi/2$ smooth lines were replaced by $\pi/2$ loaded cells. At higher order modes, smooth $\pi/2$ sections are too dispersive. We presented a design of a high power load using a disk-loaded coaxial guide operating in the TE_{01} mode. The center conductor can be internally water cooled. It has no field emission problems and its peak power carrying capacity, limited by the peak magnetic field, is 9 times that of our present load. The magnetic field could be further reduced by shaping the disk. Although we considered only DLG, operating in the TE_{01} mode, the design methods described in this note apply to any cell geometry, operating in any mode.

ACKNOWLEDGEMENT

I thank N. Baboi and C. Nantista for their help with HFSS. I am grateful to V. Dolgashev for his help with HFSS and SMART2D. His help enabled me to write this note. Jose Chan supplied Figure 14.

References

[1] S.B. Cohn, "Optimum Design of Stepped Transmission Line Transformers", IRE Trans, Vol. MTT-3, pp 16-21, April, 1995.

[2] J. L. Altman, "Microwave Circuits", Ch. 4, Van Nostrand, 1964.

[3] S. G. Tantavi, R . Vlieks "Compact X-band High Power Load Using Magnetic Stainless Steel", PAC 1995.

[4] V.A. Dolgashev, "Calculation of Impedance for Multiple Waveguide Junction Using Scattering Matrix Formulation", icap98

[5] S. G. Tantavi et. al. "The generation of 400 MW RF pulses at X-band etc", IEEE Trans, Vol. MTT-47, pp 2539-46, Dec. 1999.

[6] A.E. Atia and A. E. Williams, "General TE_{011}-mode Waveguide Bandpass Filter", IEEE Trans, Vol. MTT-24, pg. 640, Oct, 1976.

[7] C. Montgomery R. Dicke and E. Purcell "Principles of Microwave Circuits", pg. 58-59, McGraw-Hill 1948.

Appendix A

Z_{tn}	r_a [cm]	d_c[cm]	a_{pn}	d_{pz} [cm]	p_{zn}	v_g [%C]
1.3809	1.0987	0.9761	0.7915	0.3320	1.1640	56.3196
3.9304	1.4663	1.4326	0.5978	0.6441	1.7881	31.2337
11.1865	1.6526	1.6047	0.4997	0.7885	2.0770	15.2201
15.4481	1.7025	0.8162	0.4734	0.8162	2.1325	11.7421

Table 1. Parameters of the disk-loaded coax test structure or of the filter structure, up to the symmetry plane.

rg1	dg1	rg2	dg2	rg3	dg3	dm1	t1	rm1
0.750	1.25	0.856	0.222	1.123	2.38	0.098	0.079	0.4145
0.750	1.25	0.856	0.222	1.123	2.38	0.276	0.079	0.437

Table 2. Dimensions in inches of the matching section from the 1.5 inch diameter wave guide to the disk-loaded coaxial load.

	r_a [cm]	d_c[cm]	a_{pn}	d_{pz} [cm]	p_{zn}	v_g [%C]
1	1.0987	0.9761	0.7915	0.3320	1.1640	56.3196
2	1.4663	1.4326	0.5978	0.6441	1.7881	31.2337
3	1.6526	1.6047	0.4997	0.7885	2.0770	15.2201
4	1.7025	1.6373	0.8985	0.8167	2.1334	11.7199
5	1.7100	1.6484	0.8910	0.8205	2.1411	11.2489
6	1.7250	1.6626	0.8760	0.8278	2.1557	10.3426
7	1.7400	1.6761	0.8610	0.8348	2.1696	9.4848
8	1.7550	1.6889	0.8460	0.8413	2.1827	8.6758
9	1.7700	1.7009	0.8310	0.8475	2.1951	7.9158
10	1.7850	1.7123	0.8160	0.8534	2.2068	7.2047
11	1.8000	1.7230	0.8010	0.8589	2.2178	6.5419
12	1.8150	1.7331	0.7860	0.8641	2.2282	5.9265
13	1.8300	1.7425	0.7710	0.8690	2.2379	5.3575
14	1.8450	1.7515	0.7560	0.8736	2.2471	4.8333
15	1.8600	1.7599	0.7410	0.8779	2.2558	4.3521
16	1.8750	1.7678	0.7260	0.8820	2.2639	3.9118
17	1.8900	1.7753	0.7110	0.8858	2.2717	3.5098
18	1.9050	1.7825	0.6960	0.8895	2.2790	3.1434
19	1.9200	0.6350	0.6810	0.8930	2.2860	2.8095

Table 3. Parameters of the disk-loaded coax TE01 load.

Only r_a and d_c are needed for modelling and for machining.

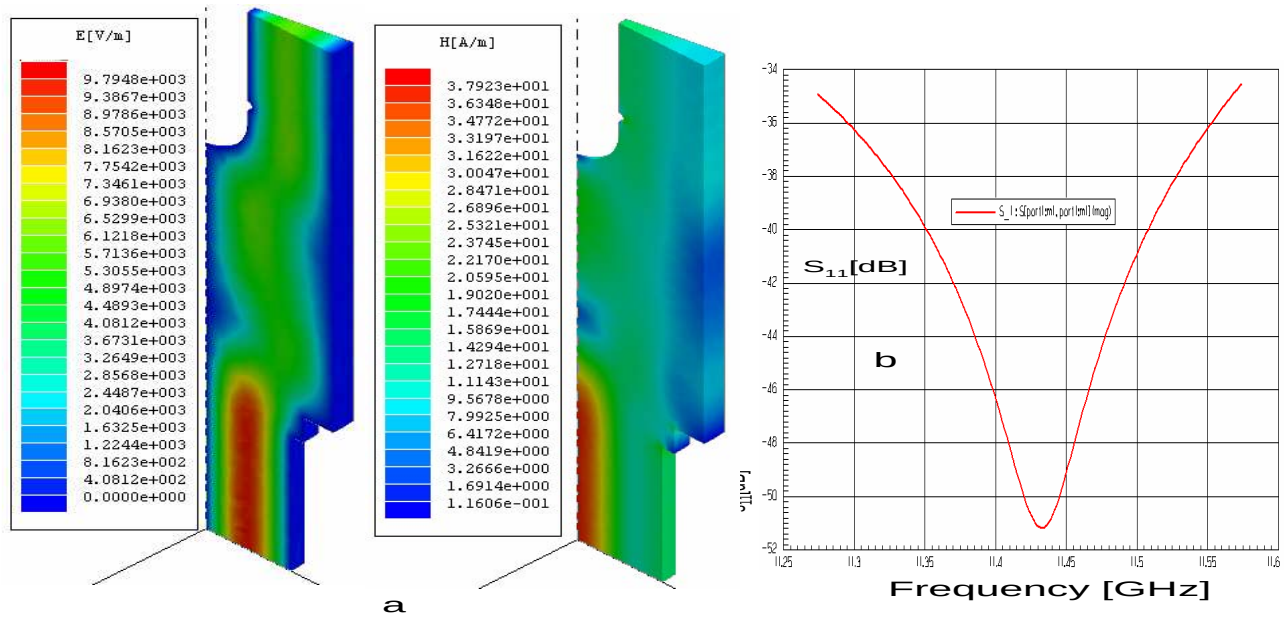

Figure 8: (a) Waveguide to coax match color plots of complex magnitude of electric and magnetic fields. (b) Its reflection.

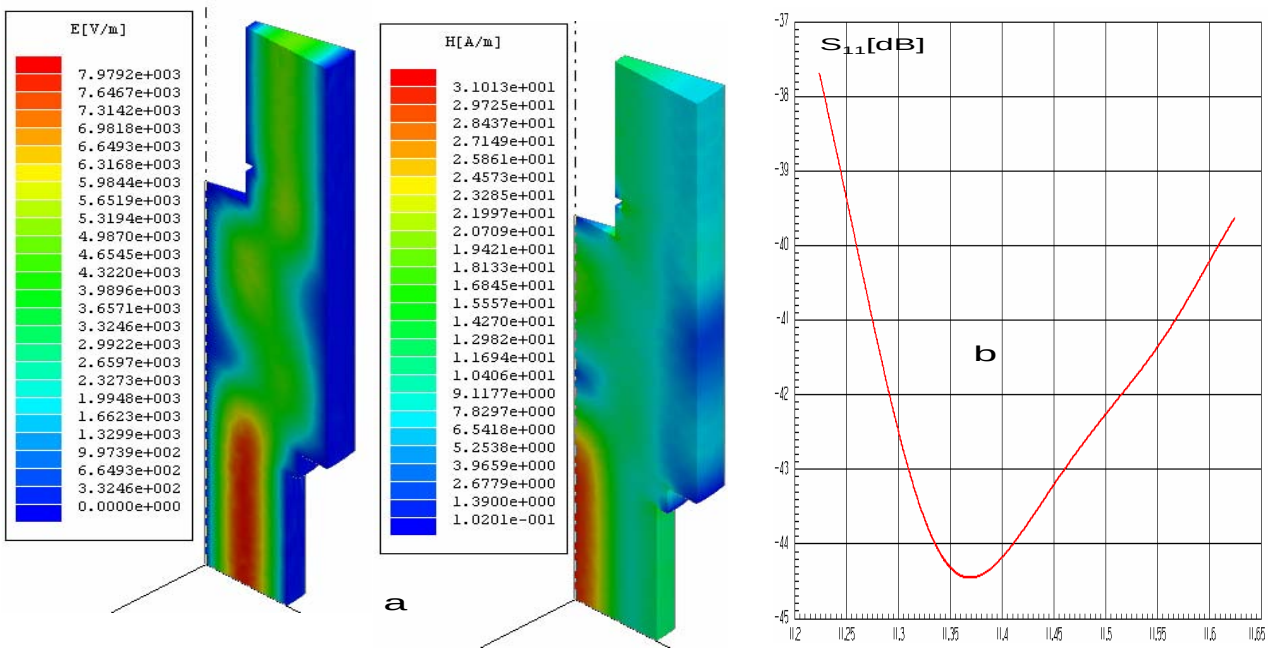

Figure 9: Alternate Design. a) Waveguide to coax match color plots of complex magnitude of electric and magnetic fields. b) Its reflection

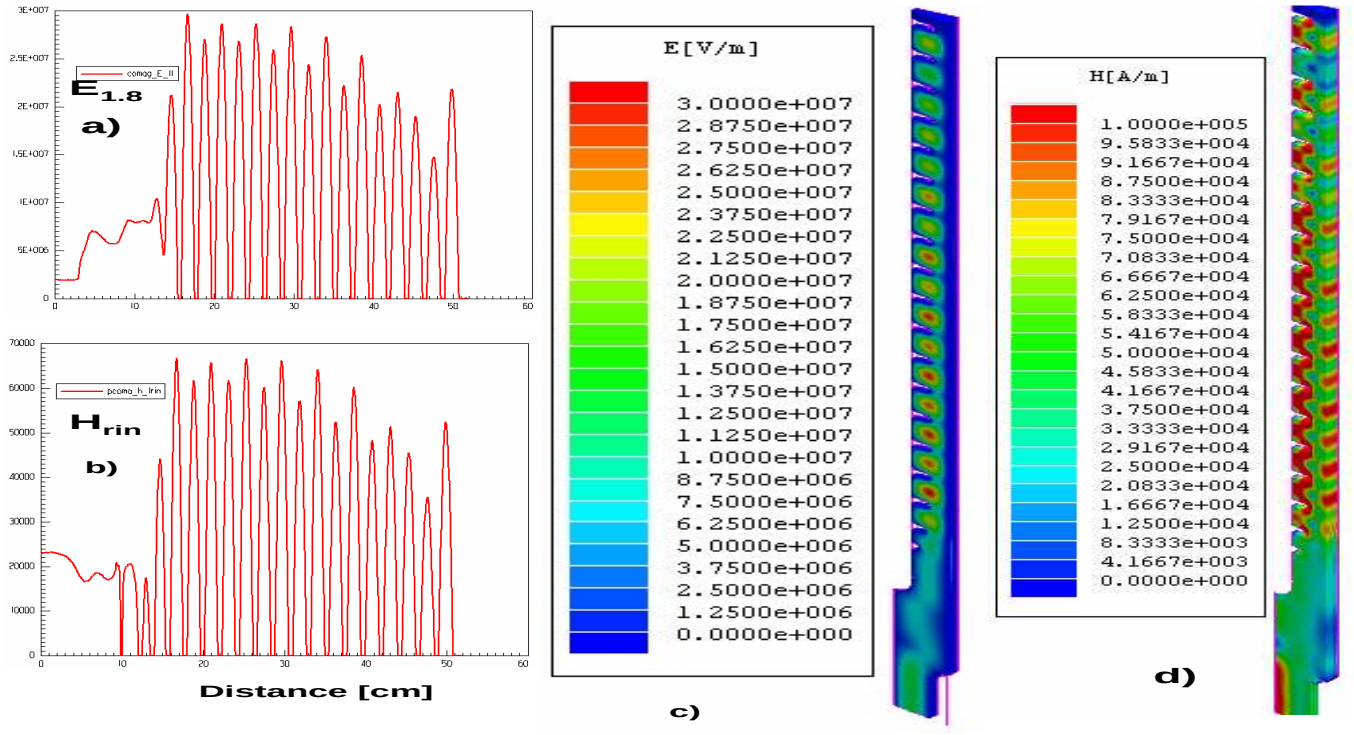

Figure 10: Load, waveguide input. $\Gamma(1) = 0.16$, a) E at=1.8 cm b) H at $r = r_{in}$ c) E color map d) H color map

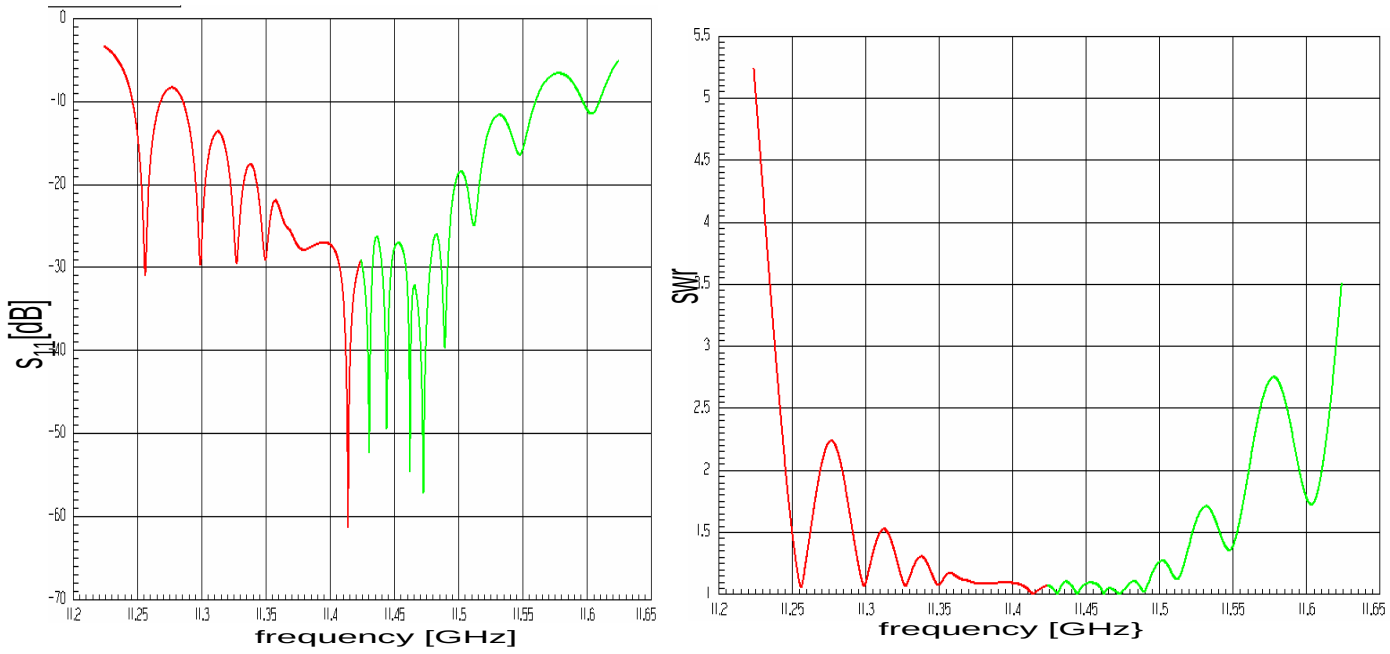

Figure 11: Load, waveguide input. Reflection and SWR. The point at the intersection of the two colors denotes the design frequency of 11.424 GHz

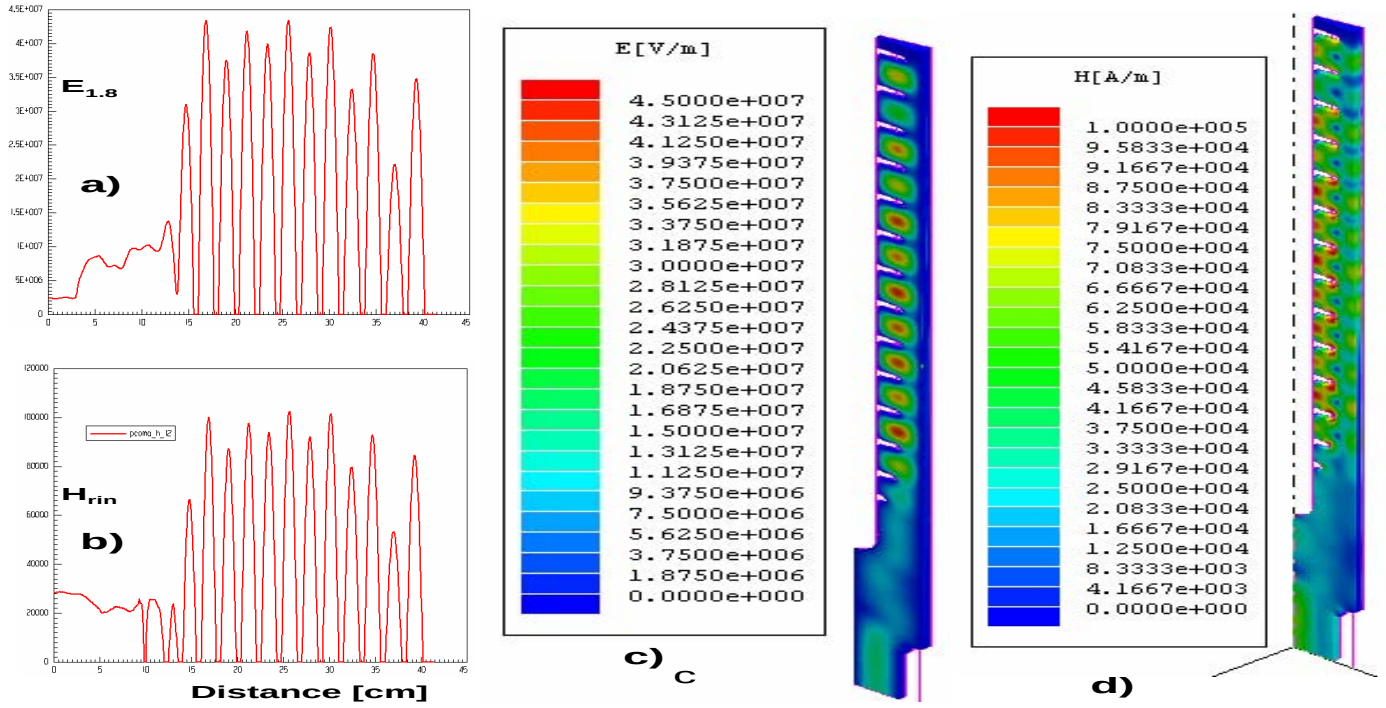

Figure 12: Load, waveguide input.$\Gamma(1) = 0.18$, a) E at r=1.8 cm b) H at $r = r_{in}$ c) E color map d) H color map

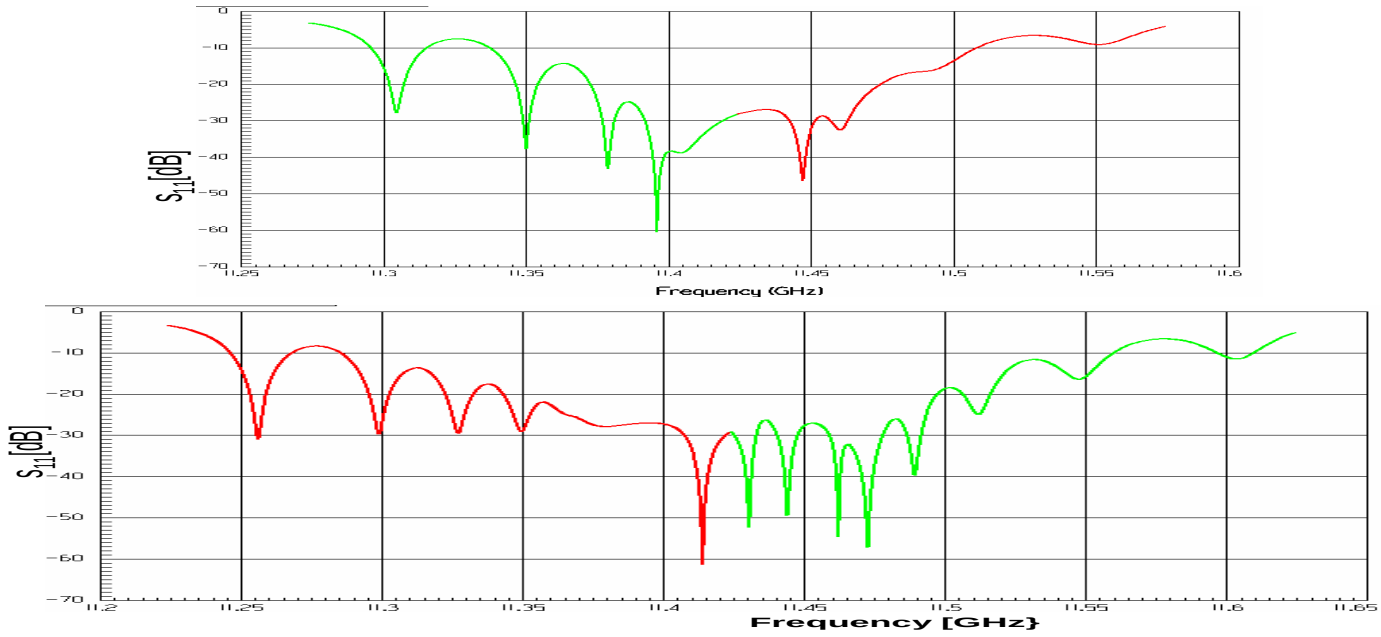

Figure 13: Comparison of reflection as a function of frequency for two load designs. The point at the intersection of the two colors denotes the design frequency of 11.424 GHz

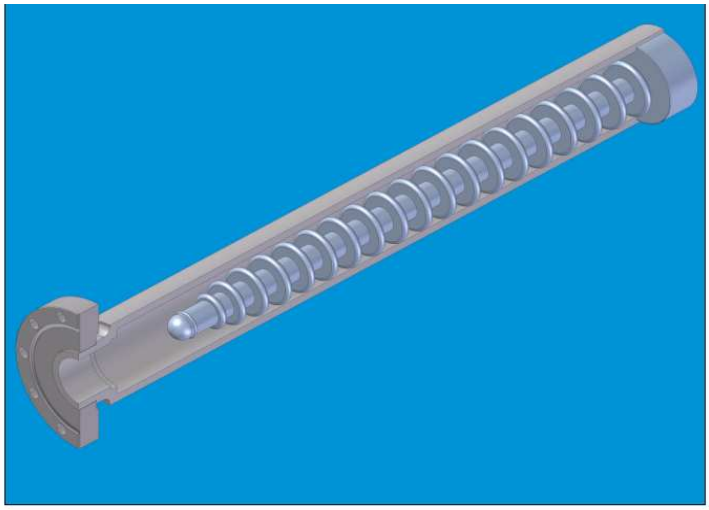

Figure 14: High Power TE_{01} Load.

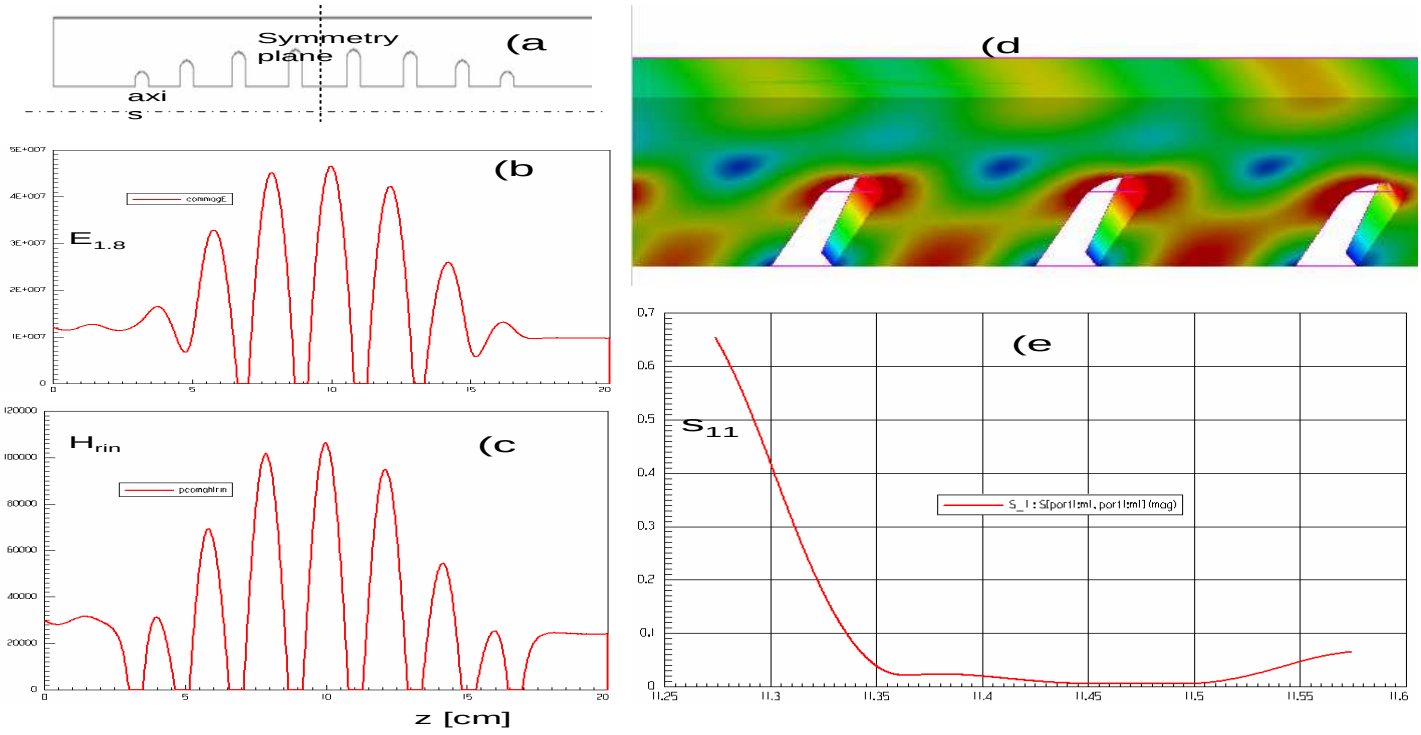

Figure 15: Test structure a) Cross section b) E at t=1.8 cm c) H at $r = r_{in}$ d) E color map e) Reflections

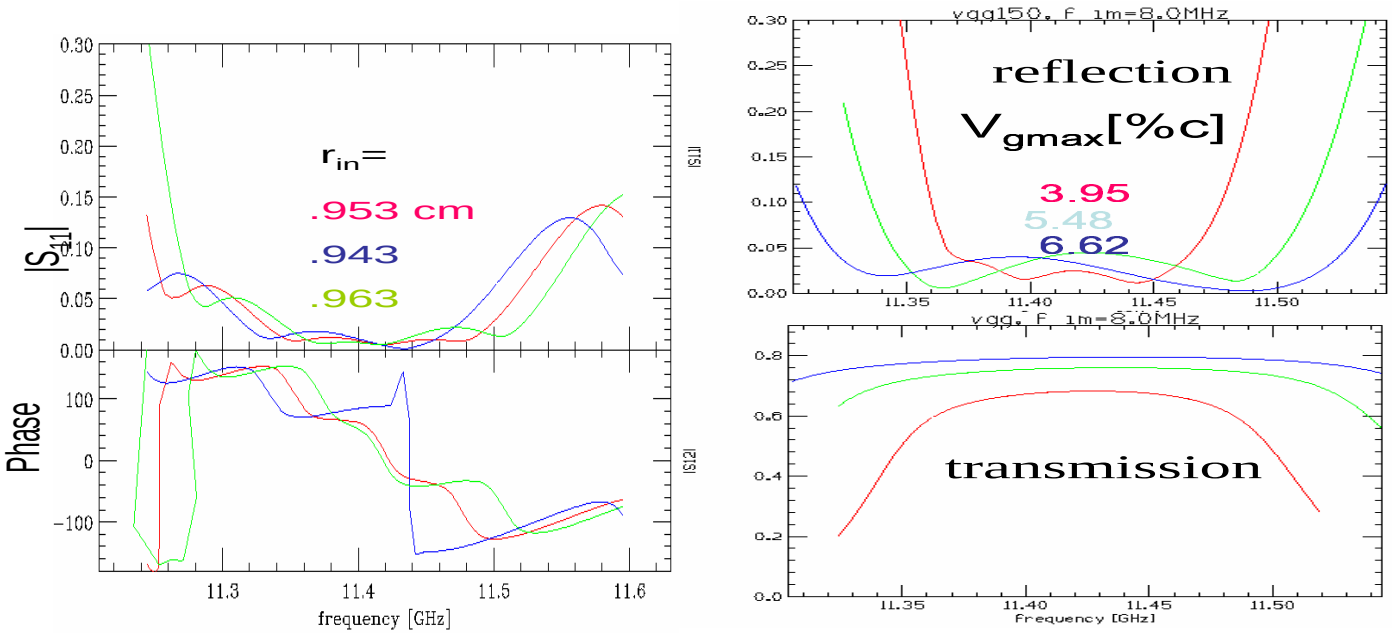

Figure 16: Test section: (a) Reflection and phase vs. frequency for three inner conductor radii. (b) Reflection and transmission vs. frequency for three group velocities.

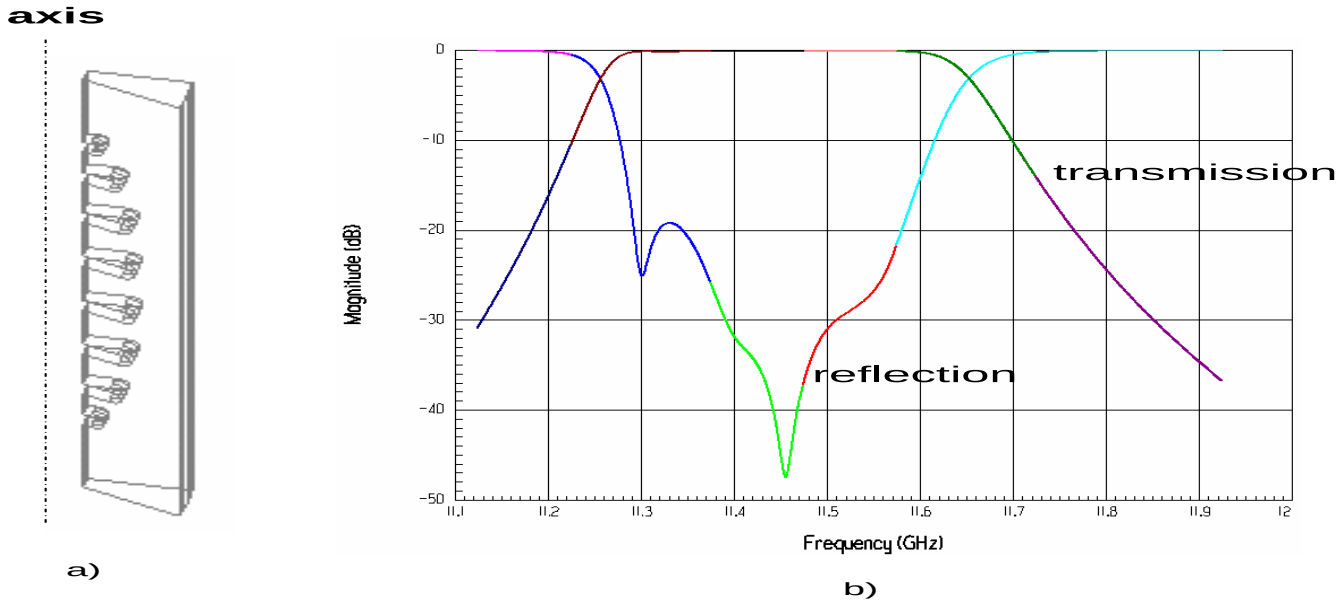

Figure 17: TE_{01} a)Coaxial filter geometry, b)reflection and transmission

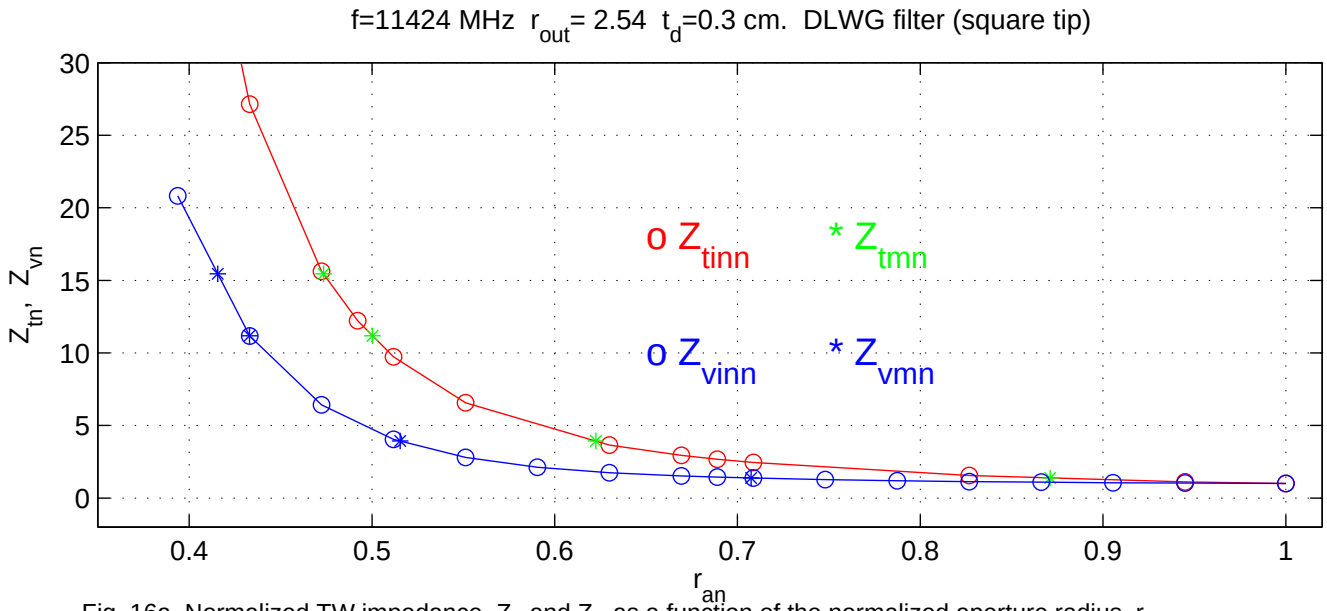

Fig. 16a. Normalized TW impedance, Z_{tn} and Z_{vn}as a function of the normalized aperture radius, r_{an}

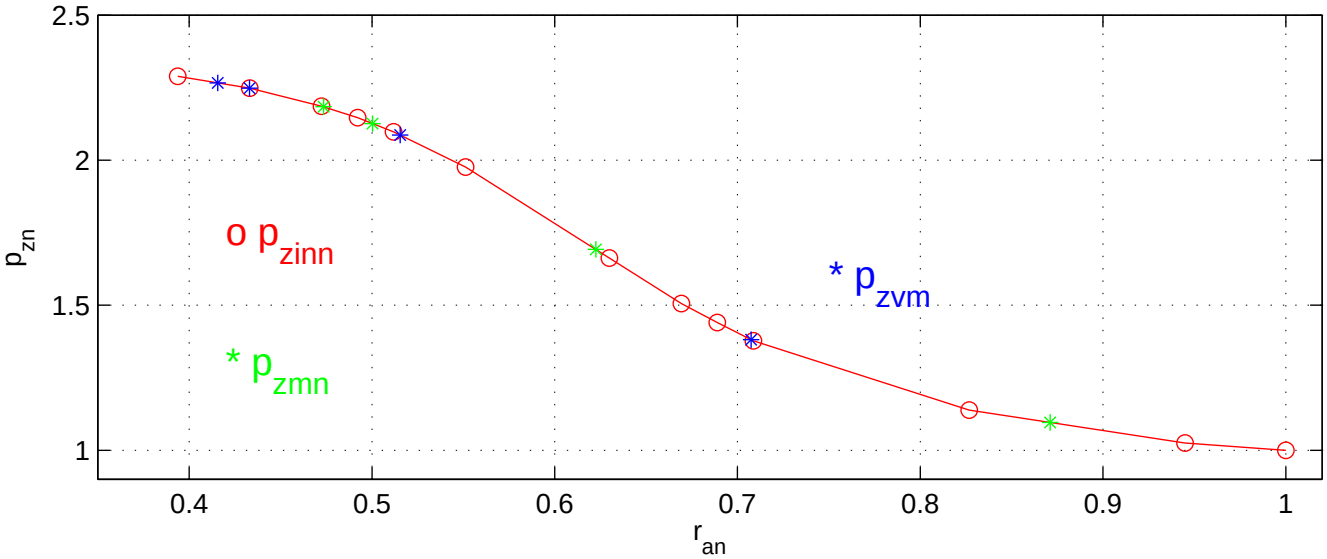

Fig. 16b. Normalized spacial period, p_{zn} as a function of normalized aperture radius r_{an}.

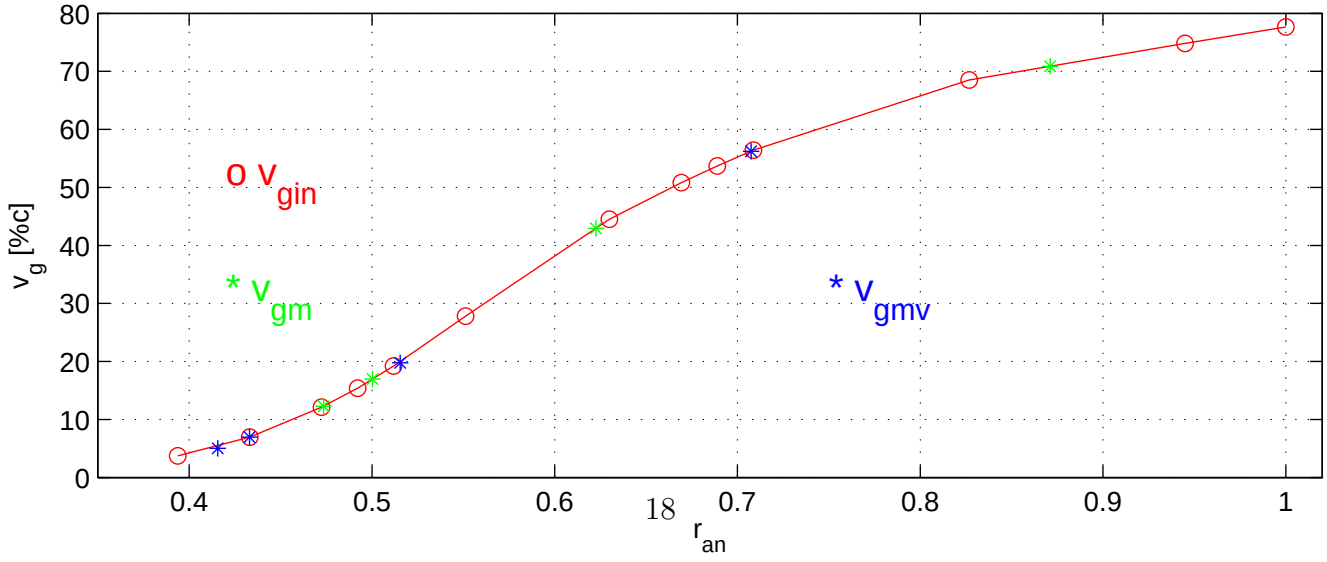

Fig. 16c. Group velocity, v_g as a function normalized aperture radius r_{an}.

Figure 18: Waveguide filter curves

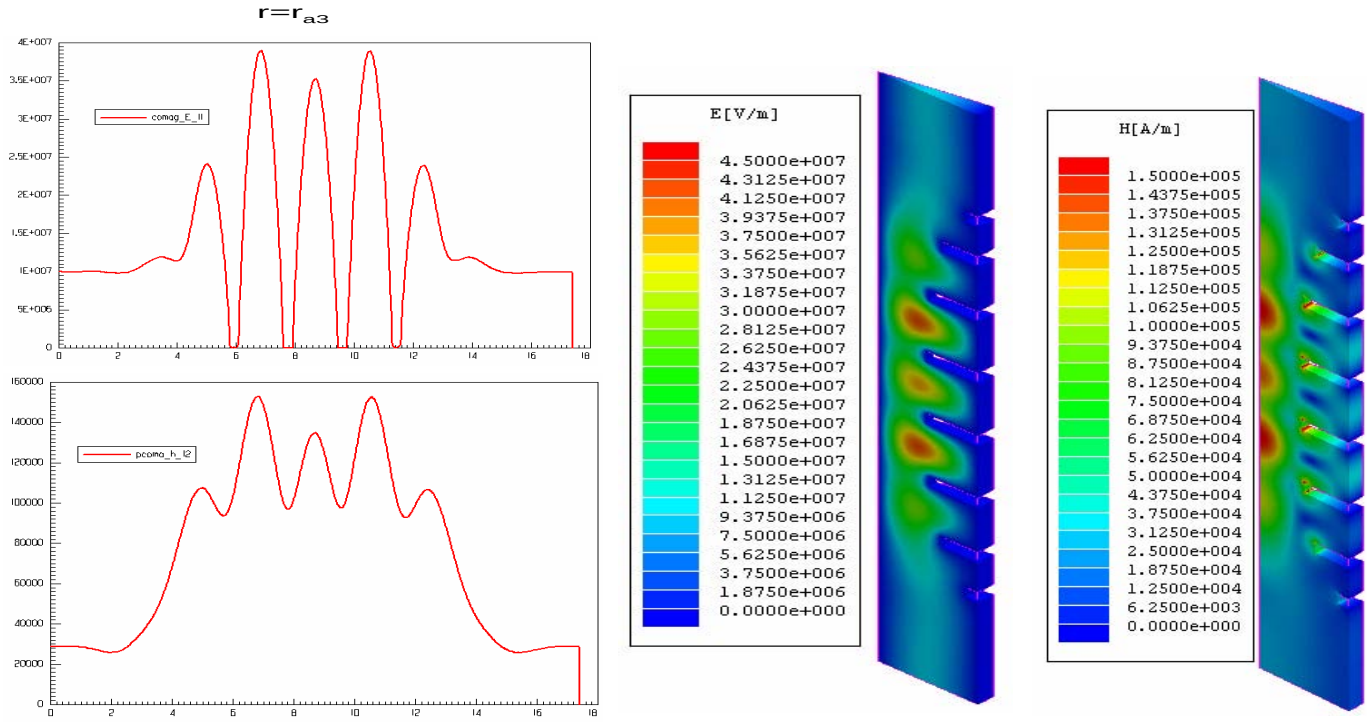

Figure 19: Load, coax input. a) E at r=1.8 cm b) H at $r = r_{in}$ c) E color map d) H color map

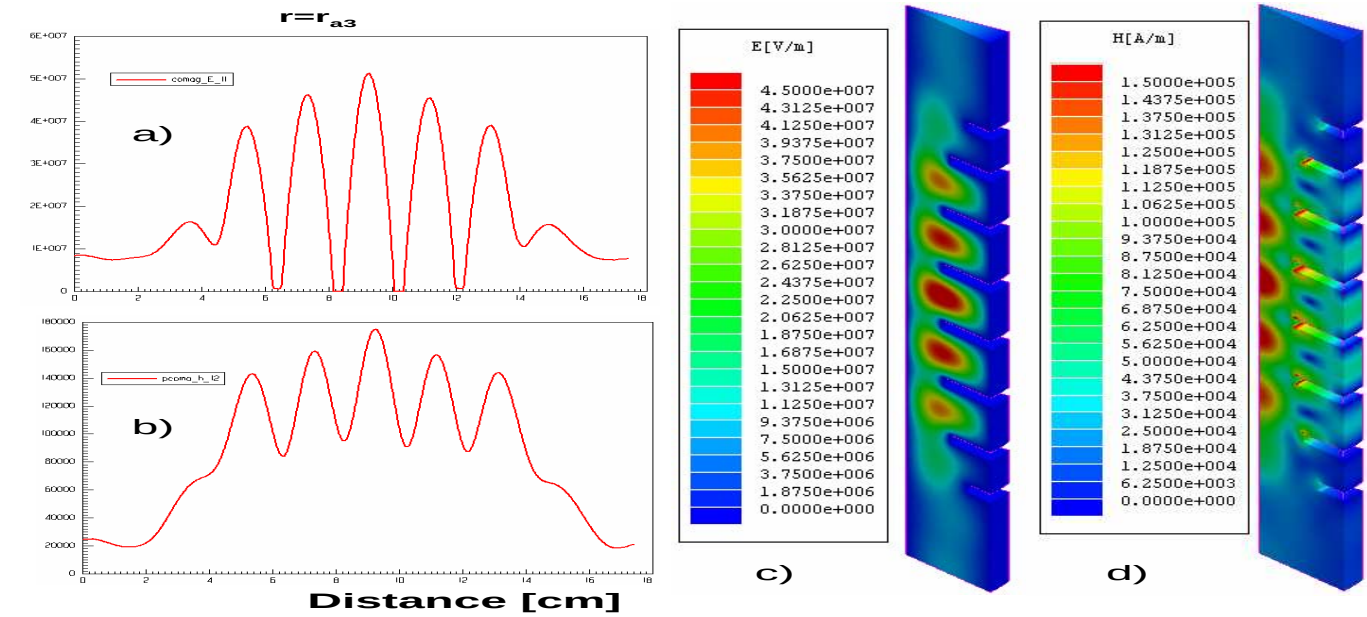

Figure 20: TE_{01} disk-loaded waveguide filter (a) E at r=1.8 cm (b) H at $r = r_{in}$ (c) E color map (d) H color map

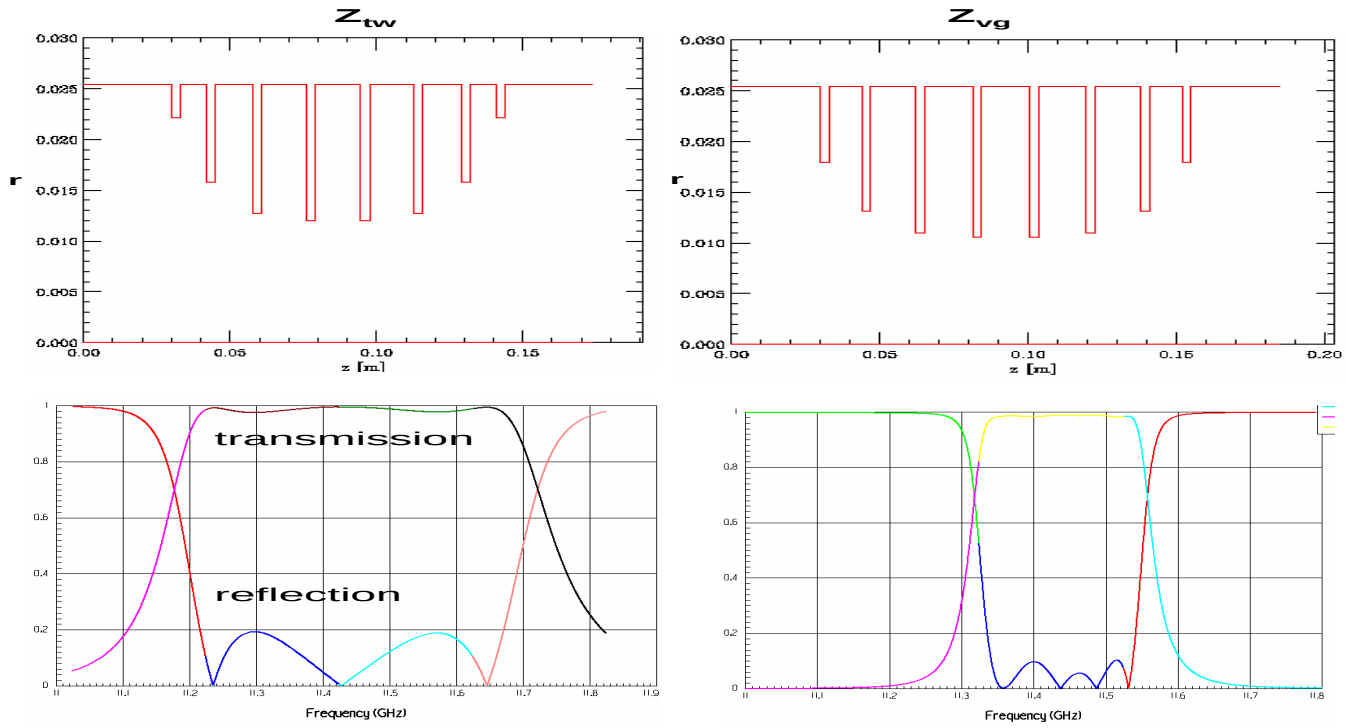

Figure 21: TE_{01} disk-loaded waveguide filter geometry, reflection and transmission as a function of frequency for two designs.

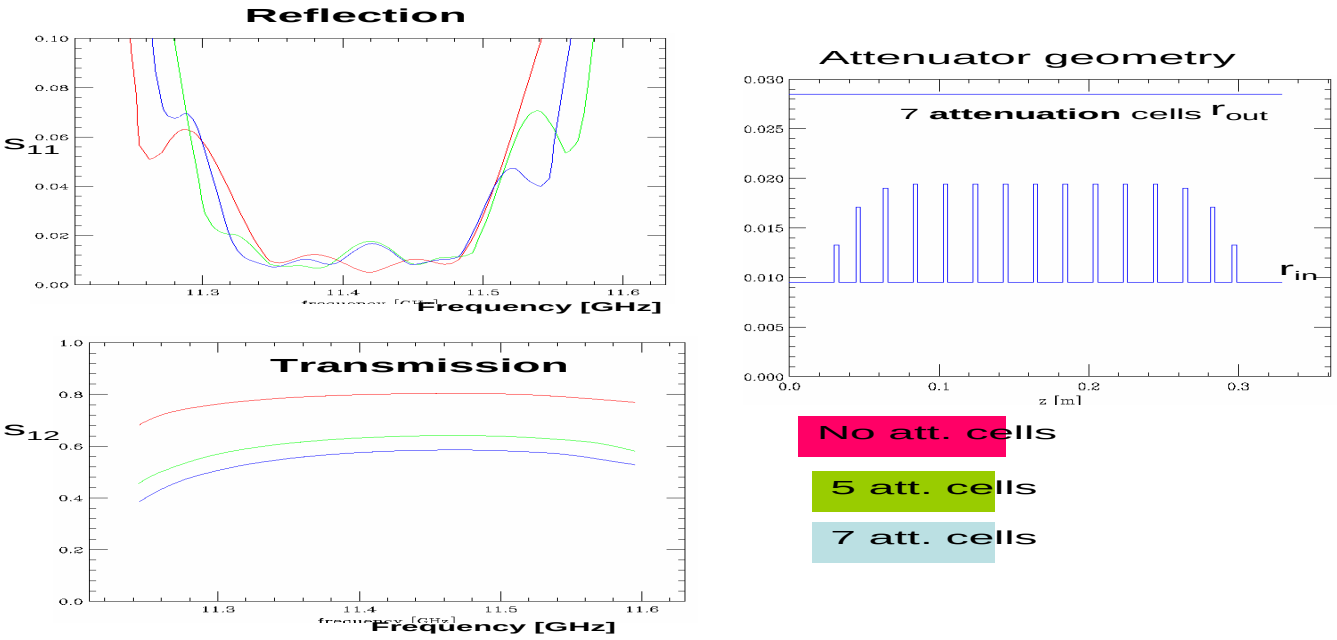

Figure 22: TE_{01} disk-loaded waveguide attenuators: geometry, reflection and transmission as a function of frequency.